PIECEWISE $H^{-1} + H^0 + H^1$ IMAGES AND THE MUMFORD-SHAH-SOBOLEV MODEL FOR SEGMENTED IMAGE DECOMPOSITION

By

Jianhong (Jackie) Shen

IMA Preprint Series # 2057

(July 2005)

INSTITUTE FOR MATHEMATICS AND ITS APPLICATIONS

UNIVERSITY OF MINNESOTA

400 Lind Hall
207 Church Street S.E.
Minneapolis, Minnesota 55455–0436

Phone: 612/624-6066 Fax: 612/626-7370
URL: http://www.ima.umn.edu

Piecewise $H^{-1} + H^0 + H^1$ Images and the Mumford-Shah-Sobolev Model for Segmented Image Decomposition *

Jianhong (Jackie) Shen
School of Mathematics, University of Minnesota, Minneapolis, MN 55455, USA

Abstract

Pattern *analysis* of naturally *synthesized* images is crucial for a number of important fields including image processing, computer vision, artificial intelligence, and computer graphics. Benefited from several important works in existence, the current research note proposes a novel free-boundary variational model for segmented image decomposition. As an inverse problem solver, the new model outputs not only the boundaries of individual objects as achieved by the Mumford-Shah model (*Comm. Pure Applied Math.,* **42**:577-685, 1989), but also a structure decomposition comprising a smooth (or cartoonish) component, an oscillatory component (or texture), and a square-integrable residue (or noise). Motivations and justifications from vision research are emphasized, and some preliminary mathematical analysis is given.

Keywords: Vision, segmentation, decomposition, texture, oscillations, free boundary.

Contents

1 Introduction: Image Modeling via Distributions

Image modeling stays at the very core of image processing and low level vision analysis. In the Bayesian framework, image modeling amounts to the introduction of suitable prior models, while in

*This work has been partially supported by the NSF (USA) under grant number DMS-0202565. Email: jhshen@math.umn.edu; Tel: (USA) (612) 625-3570.

the Tikhonov framework [44], the specification of regularity structures in order to better condition ill-posed inverse tasks such as denoising or deblurring.

In the variational approach [3, 9, 37, 38, 39], images are assumed to belong to certain function spaces on the associated continuum domain Ω (or *hypothesis classes* as in the Learning Theory [12, 40]). Common classes include (1) Sobolev spaces $W^{1,p}(\Omega)$ with $p \geq 1$, (2) the BV space $\mathrm{BV}(\Omega)$ first introduced by Rudin, Osher, and Fatemi [35, 36] and its subspace—*special BV* functions $\mathrm{SBV}(\Omega)$ [1], (3) Besov spaces $B_q^\alpha(L^p(\Omega))$ as in wavelet analysis [6, 14, 15, 26], and (4) Mumford and Shah's free-boundary model $\mathcal{H}^1(\Gamma) \oplus H^1(\Omega \mid \Gamma)$ [28, 32], where $\mathcal{H}^1(\Gamma)$ denotes the class of closed "edges" (denoted by Γ's) with finite 1-D Hausdorff measures, and $H^1(\Omega \mid \Gamma)$ Sobolev functions on $\Omega \setminus \Gamma$ for any given "edge" Γ (or using the terminology in topology and geometry, $H^1(\Omega \mid \Gamma)$ is a *fiber* at a given Γ).

Mumford remarked in 1999 (also see [31]) that it is insufficient to model images merely using *ordinary* (or equivalently, *measurable*) functions. As an alternative, *generalized* functions or *distributions* may better serve the purpose, e.g., to better reflect *scaling invariance* commonly observed in image statistics [31]. By the well known Lusin's Theorem [20], Mumford argued, a measurable function must be approximately continuous, which is a strong regularity condition hidden in all the aforementioned image models.

This notion of treating images as generalized functions was later independently rediscovered by Yves Meyer [27] in 2001 when the connection was explored between the celebrated total variation restoration model of Rudin, Osher, and Fetemi [36] and Donoho's wavelet-thresholding-based denoising [15, 16]. Meyer introduced the distributional space $\mathrm{div}(L^\infty(\Omega, \mathbb{R}^2))$ for modeling textures or oscillatory image patterns. Here the divergence operator is applied in the distributional sense: for any $\boldsymbol{g} = (g_1, g_2) \in L^\infty(\Omega, \mathbb{R}^2)$,

$$\langle \mathrm{div}\boldsymbol{g},\ \phi \rangle := -\langle \boldsymbol{g},\ \mathrm{grad}\phi \rangle, \qquad \phi \in C_0^\infty(\Omega) = D(\Omega), \quad \text{test functions.}$$

Thus generically $v = \mathrm{div}\boldsymbol{g}$ is not an ordinary measurable function.

Meyer's idea of distributional textures was soon put into practical numerical computation by Vese and Osher [45] after adopting instead the distributional spaces $\mathrm{div}(L^p(\Omega, \mathbb{R}^2))$ with $p \in [1, \infty)$. In particular, combined with the BV image model, Osher and his collaborators [34] employed the Sobolev distributional space $H^{-1}(\Omega)$ for texture processing for the first time:

$$H^{-1}(\Omega) = \mathrm{div}(L^2(\Omega, \mathbb{R}^2)). \tag{1}$$

Further discussion on $H^{-1}(\Omega)$ can be found in Section 2. We refer the reader to [4, 5, 41, 46] for some other interesting developments on mathematical texture modeling and analysis.

The current work has been closely inspired by all these remarkable works. We propose to incorporate the H^{-1}-texture component into the celebrated free-boundary segmentation model of Mumford and Shah [32]. The refined segmentation model outputs not only an optimal edge set Γ and its piecewise smooth Sobolev painting $u \in H^1(\Omega \setminus \Gamma)$, but also an H^{-1}-texture component (see Figure 1 in Section 4).

This refined segmentation model shall be called the Mumford-Shah-Sobolev model for convenience. On one hand, it perfects the Mumford-Shah model by explicitly dealing with texture patterns which were previously treated as noises. On the other hand, it provides a sound mathematical model that faithfully simulates the three key steps that a typical artist may create a painting: (i) sketching the outlines of objects in a scene (modeled by the edge set Γ), (ii) filling in the average mean-field shades (modeled by the piecewise smooth function $u \in H^1(\Omega \setminus \Gamma)$), and (iii) painting more detailed textures on each individual structure in the scene (modeled by the Sobolev distribution $v \in H^{-1}(\Omega \setminus \Gamma)$).

The organization of the paper goes as follows. Section 2 discusses the relevant Sobolev spaces as generic models for image structures. The global $H^{-1}+H^0+H^1$ image model is introduced in Section 3, and the decomposition task is formulated as an inverse problem via variational optimization. The existence and uniqueness of the optimal decomposition are established, and some mean-value properties of the optimal image components are characterized. Based on the results in Section 3, we then introduce and study piecewise $H^{-1}+H^0+H^1$ images and the Mumford-Shah-Sobolev (MSS) model for their segmented decomposition. Some limited analysis of this free-boundary variational model is developed.

This research note mainly remains in the modeling stage, supported with some preliminary mathematical analysis. We will answer many of the computational challenges in a separate forthcoming work, which is very crucial for a practical field such as computer vision. The main purpose of this research note is to bring to the attention of the mathematics community an interesting but challenging new free-boundary variational problem.

Throughout this paper, Ω represents a bounded and connected open domain in $\mathbb{R}^2$ on which images are supported. It will be called the *image domain* for convenience, and each point $x = (x_1, x_2) \in \Omega$ *a pixel*. In addition, Ω is assumed to satisfy the necessary regularity conditions (e.g., Lipschitz or the cone property) so that Poincaré-Sobolev type of inequalities hold [18, 25].

By default, we shall consistently use *parentheses* pairing (u, ϕ) to denote the L^2 integral $\int_\Omega u(x)\phi(x)dx$, and *bracket* pairing $\langle u, \phi\rangle$ to denote the dual action between $u \in D'(\Omega)$ (distribution space) and $\phi \in D(\Omega)$ (test space), or between $u \in H^{-1}(\Omega) = (H_0^1(\Omega))^*$ and $\phi \in H_0^1(\Omega)$. Without any subscripts, $\|u\|$ shall denote the ordinary L^2-norm of u. The same comments apply to vectorial functions.

2 Texture Modeling via Sobolev Distributions

In this section, we first briefly review some basic facts regarding the Sobolev spaces H^0, H^1, and H^{-1}, with special attention paid to their implications in vision research.

2.1 H^1–Images and Shift-Invariant Visual Measures

Let $D(\Omega) = C_0^\infty(\Omega)$ denote all compactly supported C^∞ test functions on Ω and $D'(\Omega)$ the collection of *distributions* or *generalized functions* on Ω which are linear functionals on $D(\Omega)$:

$$\langle u, a\phi + b\psi\rangle = a\langle u, \phi\rangle + b\langle u, \psi\rangle, \quad u \in D'(\Omega),\ \phi, \psi \in D(\Omega),\ a, b \in \mathbb{R}.$$

For instance, Dirac's delta function $u = \delta(x)$ is an important generalized function in quantum physics and signal analysis: $\langle \delta, \phi\rangle := \phi(0, 0)$, assuming that $(0, 0) \in \Omega$.

Given $u \in D'(\Omega)$, suppose $|\langle u, \phi\rangle| \le C\|\phi\|_{L^2}$ for some fixed constant C and any $\phi \in D(\Omega)$. Then Riesz's Representation Theorem reveals that u must be an ordinary *measurable* function in $L^2(\Omega)$. In the current paper, we also adopt the Sobolev notation $H^0 = H^0(\Omega)$ for $L^2(\Omega)$ (as in the title) to echo with the other two Sobolev image spaces H^1 and H^{-1} herein.

Suppose in addition that there exist two L^2 images v_1 and v_2 such that

$$\langle u, \partial_{x_i}\phi\rangle \equiv -(v_i, \phi), \quad \phi \in D(\Omega), \quad i = 1, 2.$$

Then u is said to be in the Sobolev space $H^1(\Omega)$, and its gradient is defined to be $\nabla u = (v_1, v_2) \in L^2(\Omega, \mathbb{R}^2)$. The natural inner product

$$\langle u_1, u_2\rangle_{H^1} = (u_1, u_2)_{L^2} + (\nabla u_1, \nabla u_2)_{L^2}$$

leads to the usual H^1-norm: $\|u\|_{H^1} = \sqrt{\|u\|_{L^2}^2 + \|\nabla u\|_{L^2}^2}$.

In vision research, it is interesting to adapt the H^1-norm to visual perception. Let $\|u\|_V$ denote some visual measure for an H^1-image u. It is well known that the vision system is tuned to information *variations* rather than to the *absolute intensity values* of a given image u (see, e.g., the major discovery of Nobel laureates Hubel and Wiesel [24]). One promising approach is to impose invariance under gray-level shifts:

$$\|u\|_V = \|u + \lambda\|_V, \quad \forall \ \lambda \in \mathbb{R}.$$

If sublinearity is also imposed, such a visual measure has to be a semi-norm. In fact, $\|\nabla u\|_{L^2}$ is a natural candidate, and the following theorem shows that in some sense it is the *only* one.

Theorem 1 (Shift-Invariant Visual Measure) *Let $\|u\|_V$ be a* shift-invariant *visual measure that satisfies*

$$A\|\nabla u\|_{L^2} \leq \|u\|_V \leq B\|u\|_{H^1},$$

for some fixed positive parameters A and B and all $u \in H^1(\Omega)$. Then it must be equivalent to $\|\nabla u\|_{L^2}$, i.e., there exist two constants $C > 0$ and $D > 0$ such that for any $u \in H^1(\Omega)$.

$$C\|\nabla u\|_{L^2} \leq \|u\|_V \leq D\|\nabla u\|_{L^2}.$$

Proof. One can obviously take $C = A$. On the other hand, by shift invariance,

$$\|u\|_V = \|u - \theta\|_V \leq B\|u - \theta\|_{H^1}, \quad \theta \in \mathbb{R}.$$

Take the special value

$$\theta = \langle u \rangle_\Omega := \frac{1}{|\Omega|} \int_\Omega u(x)dx.$$

By Poiecaré's inequality, there exists a fixed positive bound $K > 0$ such that

$$\|u - \langle u \rangle\|_{L^2} \leq K\|\nabla u\|_{L^2}, \quad \forall \ u \in H^1(\Omega). \tag{2}$$

Thus $\|u - \langle u \rangle\|_{H^1} \leq \sqrt{K^2 + 1}\|\nabla u\|_{L^2}$ and taking $D = B\sqrt{K^2 + 1}$ completes the proof. □

2.2 H^{-1}–Distributions and Oscillatory Textures

$H_0^1(\Omega)$ is the H^1-closure of all test functions $D(\Omega)$ in $H^1(\Omega)$. Equivalently, it consists of all H^1-images whose traces along the boundary $\partial\Omega$ vanish. $H^{-1}(\Omega)$ is the dual space of $H_0^1(\Omega)$.

Normally in the literature [18], $H_0^1(\Omega)$ inherits the norm of $H^1(\Omega)$. On the other hand, by Poincaré's inequality, there exists some positive constant $C > 0$ such that

$$\|u\|_{L^2} \leq C\|\nabla u\|_{L^2}, \quad \text{for any } u \in H_0^1(\Omega). \tag{3}$$

Thus, the homogeneous semi-norm $\|\nabla u\|_{L^2}$ is in fact a genuine norm in $H_0^1(\Omega)$, and the homogeneous bilinear form $(\nabla u_1, \nabla u_2)$ is equivalent to the H^1-inner product. These are the norm and inner product adopted in the current paper for $H_0^1(\Omega)$.

By Riesz's Representation Theorem, the dual space $H^{-1}(\Omega)$ is isomorphic to $H_0^1(\Omega)$. More specifically, given any H^{-1} texture v, there exists a unique $\Phi \in H_0^1(\Omega)$ such that for any $u \in H_0^1(\Omega)$,

$$\langle v, u \rangle = (\nabla\Phi, \nabla u).$$

As a result, one must have $v = -\Delta\Phi$ as a distribution, and the dual norm is given by

$$\|v\|_{H^{-1}} = \sup_{\|u\|_{H_0^1} \le 1} \langle v, u \rangle = \|\nabla\Phi\|_{L^2} = \|\Phi\|_{H_0^1}.$$

Notice that from the PDE point of view, the inverse problem $v \to \Phi$ is realized by the following Poisson equation with homogeneous boundary condition:

$$-\Delta\Phi = v, \quad x \in \Omega; \qquad \Phi = 0, \quad \text{along } \partial\Omega.$$

Writing $\Phi = (-\Delta)^{-1}v$, one has $\|v\|_{H^{-1}} = \|\nabla(-\Delta)^{-1}v\|_{L^2}$, as in Osher, Sole, and Vese [34].

Definition 1 (Texture Source and Potential) *As inspired by electromagnetism, v shall be called the texture or texture* source*, and Φ the texture* potential *generated by v.*

In electromagnetism, v represents the source of electric charges on Ω, and Φ the electric potential generated on Ω with a *grounded* boundary: $\Phi\big|_{\partial\Omega} = 0$.

2.3 Texture or Non-Texture

When should a given image be treated as an H^{-1}–texture? Let us elucidate the answer via a simple 1-D example.

Let $\Omega = (0, 2)$ be an interval domain, and $u_n(x) = \sin(n\pi x)$ be a sequence of harmonic waves with $n = 1, 2, \cdots$. As an H^1-image, the norm (or cost) of u_n is given by

$$\|u_n\|_{H^1} = \sqrt{\|u_n\|_{L^2}^2 + \|u_n'\|_{L^2}^2} = \sqrt{1 + (n\pi)^2}.$$

Let $\Delta = d^2/dx^2$ denote the 1-D Laplacian. Solving the homogeneous boundary–value problem

$$-\Delta\Phi_n = u_n, \qquad \Phi_n(0) = \Phi_n(2) = 0,$$

one has $\Phi_n = \sin(n\pi x)/(n\pi)^2$, and consequently,

$$\|u_n\|_{H^{-1}} = \|\nabla\Phi_n\|_{L^2} = \frac{1}{n\pi}.$$

Therefore, it is much cheaper to treat u_n's as H^{-1}–textures than H^1–structures, especially for large n's with high oscillations. Such a quantitative conclusion is consistent with the general notion in vision research that textures are small-scale features.

3 Global $H^{-1} + H^0 + H^1$ Images and Decomposition

3.1 The Model

We first consider *global* $H^{-1} + H^0 + H^1$–images and their analysis. In the next section, their *piecewise* structures are then introduced and investigated.

Consider the image formation model (or a *synthesis* model):

$$u_0(x) = u(x) + v(x) + w(x), \qquad x \in \Omega,$$

with $u \in H^1(\Omega)$, $v \in H^{-1}(\Omega)$, and $w \in H^0(\Omega) = L^2(\Omega)$. The inverse task is to decompose such a given image u_0 into a triple (u, v, w). Due to the equality constraint, only u and v are independent given any synthesized image observation u_0.

Perceptually, u represents smoother cartoonish structures and v small-scale detailed structures. Their generation mechanisms in the real world are often independent [8]. More properly handled by probability or statistical estimation theory, in particular the Bayesian principle [21, 30], the inverse decomposition $u_0 \to (u, v)$ can be achieved by maximizing the posterior probability (MAP)

$$p(u, v \mid u_0) = p(u)p(v)p(u_0 \mid u, v)/p(u_0).$$

In terms of the logarithmic likelihood $E[\cdot] = -\log p(\cdot)$, or formally the Gibbs "energy" in statistical mechanics [22], the MAP decomposition is equivalent to minimizing (up to some insignificant additive constant)

$$E[u, v \mid u_0] = E[u] + E[v] + E[u_0 \mid u, v].$$

We refer the reader to [8, 9, 30] for such Bayesian rationale to variational modeling in contemporary vision research. In summary, we consider the following variational decomposition model:

$$\min E[u, v \mid u_0] = \alpha \int_\Omega |\nabla u|^2 dx + \mu \int_\Omega |\nabla(-\Delta)^{-1} v|^2 dx + \lambda \int_\Omega (u_0 - u - v)^2 dx. \tag{4}$$

For v and w, we have adopted the measures $\|v\|_{H^{-1}}$ and $\|w\|_{L^2}$. For u, the shift-invariant *semi-norm* $\|\nabla u\|_{L^2}$ has been incorporated instead of $\|u\|_{H^1}$, which will also be denoted by $\|u\|_{\dot{H}^1}$ using the standard dot notation for homogeneous semi-norms. Also notice that only the relative ratios $\alpha : \mu : \lambda$ are essential for the optimization.

To explicitly reveal the role of certain parameters, we may also occasionally write the above energy in the form of, e.g., $E[u, v \mid u_0, \mu]$ or $E[u, v \mid u_0, \alpha, \lambda]$. As conventional in probability theory, the vertical bar separates unknown variables u, v from the given or known ones.

3.2 Uniqueness and Existence of Optimal Decomposition

We now establish the uniqueness and existence of the above decomposition model.

Lemma 1 (Weak Compactness and Lower Semi-Continuity in H^{-1}) *Suppose $(v_n)_n$ is a bounded sequence in $H^{-1}(\Omega)$. Then there must exist a subsequence $(v_{n_k})_k$ and some $v_* \in H^{-1}(\Omega)$ such that $v_{n_k} \to v_*$* weakly*, i.e., for any $\phi \in H_0^1(\Omega)$,*

$$\langle v_{n_k}, \phi \rangle \to \langle v_*, \phi \rangle, \quad k \to \infty.$$

Furthermore, $\|v_*\|_{H^{-1}} \leq \liminf_k \|v_{n_k}\|_{H^{-1}}$.

The proof is straightforward based on the $H^{-1} \leftrightarrow H_0^1$ isomorphism: $v_n \leftrightarrow \Phi_n = (-\Delta)^{-1} v_n$, and Rellich's theorem on the pre-compactness of $(\Phi_n)_n$ in $L^2(\Omega)$ [18]. (One could also apply the more general property that *any bounded sequence in a separable and reflexive Banach space has a weakly convergent subsequence.*)

We now prepare two more lemmas for the uniqueness and existence theorem to come. Let $G = G(x)$ denote the texture potential on Ω generated by the uniform texture distribution $v = 1$:

$$-\Delta G(x) = 1, \quad x \in \Omega; \qquad G(z) = 0, \quad z \in \partial\Omega.$$

In particular, $G \in H_0^1(\Omega)$, and

$$(\nabla G, \nabla G) = (G, -\Delta G) = \int_\Omega G(x)dx > 0.$$

Define $g = G/\sqrt{\int_\Omega G} = G/\|\nabla G\|$. Then with $c_0 = 1/\sqrt{\int_\Omega G} = 1/\|\nabla G\|$,

$$g = c_0 G \in H_0^1(\Omega), \quad -\Delta g = c_0, \qquad \text{and} \quad \|\nabla g\| = 1. \tag{5}$$

Lemma 2 *For any distributional texture $v \in H^{-1}(\Omega)$, one has*

$$\min_{c\in\mathbb{R}} \|v - c\|_{H^{-1}} = \|v - \langle v, g\rangle c_0\|_{H^{-1}}.$$

That is, the optimal scalar c is achieved at $c_* = \langle v, g\rangle c_0$, where $\langle v, g\rangle$ represents the coupling between $v \in H^{-1}(\Omega)$ and $g \in H_0^1(\Omega)$.

Proof. Since $(-\Delta)^{-1}(v - c) = \Phi - cG \in H_0^1(\Omega)$, one has

$$\inf_{c\in\mathbb{R}} \|v - c\|_{H^{-1}} = \inf_{c\in\mathbb{R}} \|\nabla\Phi - c\nabla G\| = \inf_{t\in\mathbb{R}} \|\nabla\Phi - t\nabla g\| = \|\nabla\Phi - (\nabla\Phi, \nabla g)\nabla g\|.$$

The last term is exactly $\|v - c_*\|_{H^{-1}}$ with

$$c_* = (\nabla\Phi, \nabla g)(-\Delta g) = \langle v, g\rangle c_0.$$

□

Lemma 3 (Hidden Symmetry of the Energy) *Given $u_0 \in H^{-1}(\Omega)$,*

$$\inf_{(u,v)\in H^1\times H^{-1}} E[u, v \mid u_0] = \inf_{(u,v)\in H^1\times H^{-1},\ \langle v,g\rangle=0} E[u, v \mid u_0],$$

where $E[u, v \mid u_0]$ is given in (4).

Proof. It suffices to show that the right hand side is no greater than the left. For any $(u, v) \in H^1(\Omega) \times H^{-1}(\Omega)$,

$$E[u, v \mid u_0] - E[u + c, v - c \mid u_0] = \mu\left(\|v\|_{H^{-1}}^2 - \|v - c\|_{H^{-1}}^2\right).$$

Let $c_* = \langle v, g\rangle c_0$ be the optimal scalar in the preceding lemma associated with v. Then

$$E[u, v \mid u_0] \geq E[u + c_*, v - c_* \mid u_0].$$

Meanwhile, it is easy to verify that $\langle v - c_*, g\rangle = 0$ because, by treating $c_0 \in H^{-1}(\Omega)$, one has

$$\langle c_0, g\rangle = \langle -\Delta g, g\rangle = (\nabla g, \nabla g) = 1.$$

This completes the proof. □

Further define $\rho \in H_0^1(\Omega)$ with $\int_\Omega \rho(x)dx = 1$ via

$$\rho(x) = c_0 g(x) = c_0^2 G(x) = \frac{G(x)}{\int_\Omega G(y)dy}. \tag{6}$$

The preceding lemma can be equivalently stated as

$$\inf_{(u,v)\in H^1\times H^{-1}} E[u, v \mid u_0] = \inf_{(u,v)\in H^1\times H^{-1},\ \langle v,\rho\rangle=0} E[u, v \mid u_0],$$

Theorem 2 (Uniqueness and Existence of Decomposition) *Given $u_0 \in H^{-1}(\Omega) + H^0(\Omega) + H^1(\Omega)\ \big(= H^{-1}(\Omega)\big)$, there exists a unique optimal decomposition $(u_*, v_*) \in H^1(\Omega) \times H^{-1}(\Omega)$ for the functional $E[u, v \mid u_0]$ in (4).*

Proof. Uniqueness follows directly from the *strict convexity* of the functional $E[u, v \mid u_0]$ in $H^1(\Omega) \times H^{-1}(\Omega)$. Strict convexity results from the following argument. Suppose for some $t \in (0, 1)$ and $(u_i, v_i)(i = 1, 2)$,

$$E[t(u_1, v_1) + (1-t)(u_2, v_2) \mid u_0] = tE[u_1, v_1 \mid u_0] + (1-t)E[u_2, v_2 \mid u_0].$$

Then the first term in the functional requires $\nabla u_1 = \nabla u_2$ a.e., or $u_1 - u_2 = const.$ Similarly the second term demands $\Phi_1 - \Phi_2 = const.$ where $\Phi_i = (-\Delta)^{-1} v_i$. The third term further requires $u_1 + v_1 = u_2 + v_2$, or $u_1 - u_2 = -(v_1 - v_2)$. Since $v_1 - v_2 = -\Delta\Phi_1 + \Delta\Phi_2 = 0$ following the second term, one must have $v_1 = v_2$ and $u_1 = u_2$, namely, the strict convexity.

Next we establish the existence of an optimal decomposition pair (u_*, v_*). By the assumption that $u_0 \in H^{-1}(\Omega)$, one must have

$$\inf E[u, v \mid u_0] \le E[u = 0, v = u_0 \mid u_0] = \mu \|u_0\|_{H^{-1}}^2 < \infty.$$

Let $(u_n, v_n) \in H^1(\Omega) \times H^{-1}(\Omega)$ be a minimizing sequence with finite energies:

$$\lim_{n\to\infty} E[u_n, v_n \mid u_0] = \inf_{(u,v)\in H^1\times H^{-1}} E[u, v \mid u_0].$$

By the preceding lemma, one can assume that $\langle v_n, \rho\rangle \equiv 0$ for $n = 1 : \infty$. Let $w_n = u_0 - u_n - v_n$ denote the L^2-noise residue. Then (w_n) is bounded in $L^2(\Omega)$, and

$$\langle u_n, \rho\rangle = \langle u_0 - w_n - v_n, \rho\rangle = \langle u_0, \rho\rangle - \langle w_n, \rho\rangle.$$

Thus the values $\langle u_n, \rho\rangle$'s must be bounded as well. Noticing that $u_n \in H^1 \subseteq L^2$, one has

$$\langle u_n, \rho\rangle = (u_n, \rho) = \int_\Omega u_n \rho. \tag{7}$$

Since $\int_\Omega \rho = 1$, the generalized Poincaré's inequality [25] over $\Omega \subseteq \mathbb{R}^2$

$$\|u - \int_\Omega u\rho\| \le C\|\nabla u\|$$

must hold for some fixed $C > 0$ and any $u \in H^1(\Omega)$. Combined with Eqn. (7) and the fact that $\alpha\|\nabla u_n\|^2 \le E[u_n, v_n \mid u_0]$, Poincaré's inequality implies that (u_n) must be bounded in $H^1(\Omega)$. Then by the compactness theorem of Rellich and Kondrachov [18], there is a subsequence of (u_n, v_n), for convenience still denoted by (u_n, v_n) (and thus the old sequence is dumped from this point on), and some $u_* \in H^1(\Omega)$, such that $u_n \to u_*$ in $L^2(\Omega)$, and the lower semi-continuity property holds:

$$\|\nabla u_*\| \le \liminf_{n\to\infty} \|\nabla u_n\|. \tag{8}$$

By Lemma 1, possibly with another round of subsequence refinement, one could assume that $v_n \to v_*$ weakly in $H^{-1}(\Omega)$ and

$$\|v_*\|_{H^{-1}} \le \liminf_{n\to\infty} \|v_n\|_{H^{-1}}. \tag{9}$$

As a result of the convergence of $(u_n, v_n)_n$, the L^2-noise residues $w_n = u_0 - u_n - v_n$ must converge to $w_* = u_0 - u_* - v_*$ in *distribution*. Since test functions are dense in $L^2(\Omega)$, one must have

$$\|w_*\| \leq \liminf_{n\to\infty} \|w_n\|. \tag{10}$$

In combination, these last three inequalities imply that

$$E[u_*, v_* \mid u_0] \leq \liminf_{n\to\infty} E[u_n, v_n \mid u_0],$$

and that (u_*, v_*) must be the (unique) minimizing pair. □

Let $\langle w \rangle$ denote the mean value of $w \in L^1(\Omega)$:

$$\langle w \rangle = \frac{1}{|\Omega|} \int_\Omega w(x) dx.$$

Some mean-values properties of the optimal decomposition are characterized next.

Theorem 3 (Mean Values of Optimal Decomposition) *Let* $(u_*, v_*) = \text{argmin } E[u, v \mid u_0]$ *for a given image* $u_0 \in H^{-1}(\Omega)$*. Then*

$$\langle u_0 - v_* \rangle = \langle u_* \rangle \qquad \textit{and} \quad \langle (-\Delta)^{-1} v_* \rangle = 0.$$

Proof. Since $w_* = u_0 - v_* - u_* \in L^2(\Omega)$, one has $U_* = u_0 - v_* = w_* + u_* \in L^2(\Omega)$, and $\langle U_* \rangle$ is well defined as a result. Given U_*, one must have

$$u_* = \text{argmin}_u \;\; \alpha \|\nabla u\|^2 + \lambda \|U_* - u\|^2.$$

After adding a shift parameter θ, one has

$$(u_*, 0) = \underset{(u,\theta)}{\text{argmin}} \; \alpha \|\nabla u\|^2 + \lambda \|U_* - u - \theta\|^2.$$

In particular,

$$0 = \text{argmin}_\theta \;\; \|U_* - u_* - \theta\|^2.$$

By the general principle of least-square approximation [42], one thus must have

$$0 = \langle U_* - u_* \rangle,$$

which yields the first identity in the theorem.

By the preceding lemma and theorem, one must have $\langle v_*, G \rangle = 0$, where $G = (-\Delta)^{-1} 1$ as defined earlier. Therefore,

$$0 = \langle v_*, (-\Delta)^{-1} 1 \rangle = \langle (-\Delta)^{-1} v_*, 1 \rangle = |\Omega| \; \langle (-\Delta)^{-1} v_* \rangle,$$

which is precisely the second identity. □

3.3 PDE Characterization of Optimal Decomposition

In this section, we characterize the optimal decomposition (u_*, v_*) by the partial differential equations (PDEs) they satisfy, or equivalently, the Euler-Lagrange equations associated with the energy.

Proposition 1 (Potential–Noise Identity) *Let $(u_*, v_*) = \operatorname{argmin}_{(u,v)} E[u, v \mid u_0]$ be the unique minimizer in $H^1(\Omega) \times H^{-1}(\Omega)$. Then the "noise"-component $w_* = u_0 - u_* - v_*$ is identical to the* potential *of the texture source v_* up to a multiplicative constant. More specifically, one has $-\beta \Delta w_* = v_*$ for $\beta = \lambda/\mu$.*

Proof. Let $\Phi_* = (-\Delta)^{-1} v_* \in H_0^1(\Omega)$ denote the potential of v_*. Consider the perturbation $v_* \to v_* + \delta v$ with $\delta v \in H^{-1}(\Omega)$. Let $\delta\Phi = (-\Delta)^{-1}\delta v$ be the corresponding potential, which is a perturbation to the optimal potential Φ_*. With u_* fixed, one has, at (u_*, v_*),

$$\delta E[u_*, v \mid u_0] = \mu \delta \left(\|\nabla \Phi\|^2 \right) + \lambda \delta \left(\|w\|^2 \right),$$

where $w = u_0 - u_* - v$ denotes the *noise*-component. Notice that

$$\delta \left(\|\nabla \Phi\|^2 \right) = 2\langle \nabla \Phi_*, \nabla \delta\Phi \rangle = 2\langle \Phi_*, -\Delta \delta\Phi \rangle = 2\langle \Phi_*, \delta v \rangle,$$

where the last two expressions denote the dual action between $H_0^1(\Omega)$ and $H^{-1}(\Omega)$. Similarly, under $v_* \to v_* + \delta v$, one has $\delta w = \delta(u_0 - u_* - v) = -\delta v$, and

$$\delta \left(\|w\|^2 \right) = 2\langle w_*, \delta w \rangle = -2\langle w_*, \delta v \rangle.$$

In combination, one must have

$$\langle \mu \Phi_* - \lambda w_*, \delta v \rangle = 0,$$

for any admissible δv. Thus the following potential–noise relation must hold:

$$\mu \Phi_* - \lambda w_* = 0, \quad \text{or} \quad \Phi_* = \beta w_* \quad \text{with} \quad \beta = \lambda/\mu. \tag{11}$$

In particular, $-\beta \Delta w_* = v_*$. This completes the proof. □

Theorem 4 (System of Euler-Lagrange Equations) *Let*

$$(u_*, v_*) = \operatorname{argmin}_{(u,v)} E[u, v \mid u_0],$$

and let $w_* = u_0 - u_* - v_*$ denote the noise residue. Then the following system of PDEs hold in the distributional sense:

$$\begin{cases} \alpha \Delta u_* + \lambda w_* = 0, \\ \lambda \Delta w_* + \mu v_* = 0, \end{cases} \tag{12}$$

with boundary conditions $\partial u_*/\partial \boldsymbol{n} = 0$ and $w_* = 0$ along $\partial\Omega$. In particular, $u_* \in H^1(\Omega)$ must belong to $H^3_{\text{loc}}(\Omega)$. Furthermore, if the given image $u_0 \in L^2(\Omega)$ and $\partial\Omega$ in C^2, then $w_* \in H_0^1(\Omega)$ in fact must belong to $H^2(\Omega)$.

Proof. The second equation and its boundary condition come directly from the preceding proposition. For the first one, one applies the perturbation $u_* \to u_* + \delta u$ with v_* fixed and $\delta u \in H^1(\Omega)$. Then $\delta w = -\delta u$, and

$$\frac{1}{2}\delta E[u, v_* \mid u_0] = \alpha \langle \nabla u_*, \nabla \delta u \rangle + \lambda \langle w_*, -\delta u \rangle = \langle -\alpha \Delta u_* - \lambda w_*, \delta u \rangle + \int_{\partial\Omega} (\boldsymbol{n} \cdot \nabla u) \delta u ds,$$

Since $\delta u \in H^1(\Omega)$ is arbitrary, one must have

$$\alpha \Delta u_* + \lambda w_* = 0 \quad \text{on } \Omega, \qquad \text{and} \quad \boldsymbol{n} \cdot \nabla u = 0 \quad \text{along } \partial\Omega,$$

which are the first equation and its boundary condition.

Concerning the regularities, $v_* \in H^{-1}(\Omega)$ implies that its potential $\beta w_* \in H_0^1(\Omega)$. Then by the theory of elliptic equations (e.g., [18]), the first (Poisson) equation implies that the weak solution $u_* \in H^1(\Omega)$ in fact must belong to $H^3_{\text{loc}}(\Omega)$ regardless of the regularity of Ω.

Furthermore, if the given image $u_0 \in L^2(\Omega)$, then the optimal texture component

$$v_* = u_0 - u_* - w_*$$

must belong to $L^2(\Omega)$ as well since $u_* \in H^1(\Omega)$ and $w_* \in L^2(\Omega)$. Then by the theory of second-order elliptic equations (e.g., [18]), if $\partial\Omega$ is a C^2-manifold, one must have $w_* = (-\Delta)^{-1} v_* \in H^2(\Omega)$. This completes the proof. □

4 Piecewise $H^{-1} + H^0 + H^1$ Images and the MSS Model

4.1 Piecewise $H^{-1} + H^0 + H^1$ Images and the MSS Model

The 3-D world is an ensemble of individual objects, or 3-D structures. Each structure has relatively homogeneous surface geometry or reflectance. As a result, under some common lighting conditions, the acquired 2-D images must also consist of various homogenous patches, each of which captures a relatively uniform 3-D pattern such as a tree, a pond, or an automobile. This view offers a heuristic foundation for adopting the class of piecewise $H^{-1} + H^0 + H^1$ images as a generic image model. Each $H^{-1} + H^0 + H^1$ piece models the image of some homogeneous 3-D object.

Given a piecewise $H^{-1} + H^0 + H^1$ image u_0, the goals of segmented decomposition are:

(1) to partition the entire image domain Ω into disjoint homogeneous patches $\Omega_1 \cup \Omega_2 \cup \ldots$, and

(2) on each patch Ω_k, to decompose the given observed image u_0 into

$$(u_k, v_k, w_k) \in H^1(\Omega_k) \times H^{-1}(\Omega_k) \times H^0(\Omega_k).$$

When the disjoint patches are defined as the connected components of $\Omega \setminus \Gamma$ for some relatively closed "curve" Γ, the above two tasks can be naturally combined to yield a free-boundary optimization problem:

$$\min E[\Gamma, u, v \mid u_0] = E[\Gamma] + E[u, v \mid \Gamma] + E[u_0 \mid u, v, \Gamma].$$

As in the preceding section, this "energy" formulation has been formally based upon the Bayesian formula [8]:

$$p(\Gamma, u, v \mid u_0) = p(\Gamma) p(u, v \mid \Gamma) p(u_0 \mid u, v, \Gamma) / p(u_0),$$

and Gibbs' energy formula $E[\cdot] = -\log p(\cdot)$. (Notice that $p(u_0)$ is merely a probability normalization constant given u_0.) Define $w = u_0 - u - v$ to be the noise residue. Coupled with the 1-D Hausdorff measure $\mathcal{H}^1$ for the edge set Γ, the $H^{-1} + H^0 + H^1$ image model of the preceding section leads to the energy formula:

$$E[\Gamma, u, v \mid u_0] = \mathcal{H}^1(\Gamma) + \alpha \|u\|^2_{\dot{H}^1(\Omega\setminus\Gamma)} + \mu \|v\|^2_{H^{-1}(\Omega\setminus\Gamma)} + \lambda \|w\|^2_{H^0(\Omega\setminus\Gamma)}, \tag{13}$$

or more explicitly,

$$E[\Gamma, u, v \mid u_0] = \mathcal{H}^1(\Gamma) + \alpha \int_{\Omega\setminus\Gamma} |\nabla u|^2 dx + \mu \int_{\Omega\setminus\Gamma} |\nabla(-\Delta_\Gamma)^{-1} v|^2 dx + \lambda \int_{\Omega\setminus\Gamma} (u_0 - u - v)^2 dx. \quad (14)$$

Notice that here the texture potential $\Phi = (-\Delta_\Gamma)^{-1} v$ is defined by

$$\Delta\Phi = v, \quad x \in \Omega \setminus \Gamma; \qquad \Phi(z) = 0, \quad z \in \partial\Omega \cup \Gamma. \quad (15)$$

Since the classical Mumford-Shah segmentation model can be derived as the asymptotic limit of the above model as $\mu \to \infty$, for convenience we simply call (13) or (14) the *Mumford-Shah-Sobolev* (MSS) model for *segmented decomposition*. Notice that all the three energies on image patches are imposed via Sobolev measures.

The existence of a minimizer to the MSS model is more involved than the corresponding problem for the classical Mumford-Shah (MS) model and will be addressed elsewhere. We refer the reader to the remarkable works of [13, 23, 28] for the MS model. The proof for the one-dimensional case is however much simpler and can be found in [8], for example.

Due to the lack of convexity in the MSS model, uniqueness is generally unguaranteed. The following construction gives an explicit example.

Consider the 1-D situation in which an edge set Γ becomes a discrete set of points and the 1-D Hausdorff measure $\mathcal{H}^1(\Gamma)$ is replaced by the atomic counting measure $\mathcal{H}^0(\Gamma)$.

Let $\Omega = (0, 1)$ be the image domain and $u_0 = 1_{(0,1/2)}(x) - 1_{[1/2,1)}(x)$ the observed image (which is the Haar mother wavelet in wavelet theory [14, 43]). Define

$$A = A(m, l) = \inf_{(u,v)\in H^1(\Omega)\times H^{-1}(\Omega)} \int_\Omega |\nabla u|^2 dx + m \int_\Omega |\nabla(-\Delta)^{-1} v|^2 dx + l \int_\Omega (u_0 - u - v)^2 dx.$$

By the existence theorem in the preceding section, there exists some $(u_*, v_*) \in H^1(\Omega) \times H^{-1}(\Omega)$ such that $A(m, l) = E[u_*, v_* \mid u_0, m, l]$. Then one must have $A(m, l) > 0$. Otherwise, the three terms in the energy would demand $u_* = const.$, $v_* = 0$, and $u_0 - u_* - v_* = const.$, which is an impossible scenario given u_0.

For any given $m, l > 0$, define

$$\alpha = \frac{1}{A(m, l)}, \quad \mu = \frac{m}{A(m, l)}, \quad \text{and} \quad \lambda = \frac{l}{A(m, l)}.$$

Theorem 5 (Nonuniqueness) *The minimizers to the MSS model $E[\Gamma, u, v \mid u_0, \alpha, \mu, \lambda]$ are nonunique given the above u_0 and any triple (α, β, λ) in the preceding formula.*

Proof. It suffices to show that the two distinct solutions,

$$(\Gamma = \text{empty set}, u = u_*, v = v_*) \quad \text{and} \quad (\Gamma = \{1/2\}, u = u_0, v = 0),$$

both achieve the minimum energy $\inf E[\Gamma, u, v \mid u_0, \mu, \lambda] = 1$. We leave the detail of this calculation as an exercise. □

4.2 Euler-Lagrange Equations for the Free-Boundary MSS

For a practical discipline such as computer vision, the actual computation of the proposed model is no less important than proper modeling and model analysis. Classical variational models are generally computed via their Euler-Lagrange equations or the gradient descent approach [8], as in

the case of the Rudin-Osher-Fatemi [36, 7] model and the Mumford-Shah model [10, 32, 17, 28]. We shall discuss the *actual* numerical analysis and implementation (via the level-set method [10, 33] and Γ-convergence [2, 17]) of the proposed MSS model in a separate work. Below we only briefly discuss the associated Euler-Lagrange equations of the MSS model.

Denote $E[\Gamma, u, v \mid u_0]$ by $E[\Gamma \mid u_0, u, v]$ when u and v are given, and $E[u, v \mid u_0, \Gamma]$ when Γ is given. Define $\Phi = (-\Delta_\Gamma)^{-1} v$ to be the Γ-segmented texture potential as in (15) and $w = u_0 - u - v$ the noise residue. Introduce the energy "density" function

$$e(x) = e(x \mid \Gamma) = \alpha |\nabla u|^2 + \mu |\nabla \Phi|^2 + \lambda w^2.$$

Then the MSS energy is given by

$$E[\Gamma, u, v \mid u_0] = \mathcal{H}^1(\Gamma) + \int_{\Omega \setminus \Gamma} e(x \mid \Gamma) dx.$$

As commonly practiced in the literature [8, 29, 36], to obtain the formulae of the Euler-Lagrange equations, the patterns (i.e., Γ, u, v, and u_0) involved are all assumed to be sufficiently regular and allow continuous differentiations. As a free-boundary problem, first consider a local perturbation $x \to x + \delta x$ of the edge feature Γ near any of its regular point, with other conditionally optimal image patterns (i.e., u, v) continuously adapted to such perturbation. The calculation leads to the first variation formula of the energy (see, e.g, [17, 32, 29])

$$\delta E = \int_\Gamma (-\kappa \boldsymbol{n} - [e]_{\boldsymbol{n}} \boldsymbol{n}) \cdot \delta x ds,$$

where ds stands for the arc length element along Γ, $\boldsymbol{n}$ the unit normal, and κ the curvature scalar coupled with $\boldsymbol{n}$ so that $\kappa \boldsymbol{n}$ points toward the center of curvature. The jump $[e]_{\boldsymbol{n}}$ is defined as

$$[e]_{\boldsymbol{n}}(x) = \lim_{\varepsilon \to 0^+} e(x + \varepsilon \boldsymbol{n}) - e(x - \varepsilon \boldsymbol{n}).$$

Thus a gradient-descent evolution equation for the curve is given by

$$\frac{\partial x}{\partial t} = \kappa \boldsymbol{n} + [e]_{\boldsymbol{n}} \boldsymbol{n}. \tag{16}$$

Notice that due to the coupling between κ and $\boldsymbol{n}$, as well as $[e]_{\boldsymbol{n}}$ and $\boldsymbol{n}$, the right-hand side does not depend upon the binary choice of $\boldsymbol{n}$. The first term is the familiar mean-curvature motion [19].

Given a current estimator Γ, the variations on the image patterns u and v on $\Omega \setminus \Gamma$ lead to the same Euler-Lagrange equations as in the preceding section. That is,

$$\begin{cases} \alpha \Delta u + \lambda w = 0, \\ \lambda \Delta w + \mu v = 0, \end{cases} \tag{17}$$

with the boundary conditions $\partial u / \partial \boldsymbol{n} = 0$ and $w = 0$ along $\partial \Omega \cup \Gamma$.

Any practical computational scheme (see, e.g., [11]) usually approaches the (local or global) minima by alternating between Eqn. (16) and (17). Starting with any initial guess of the edge set, one first solves the segmented decomposition problem (17) to obtain the optimal u and v associated to the current edge estimator Γ_t, and then applies the evolution equation (16) for some time step Δt to update the edge estimator to a new one $\Gamma_{t+\Delta t}$. Numerically such algorithm can be carried out by the level-set technology [10, 33] or the Γ-convergence approximation approach [2, 17]. We shall detail the computational issues elsewhere and Fig. 1 shows the performance of the MSS model on a natural test image.

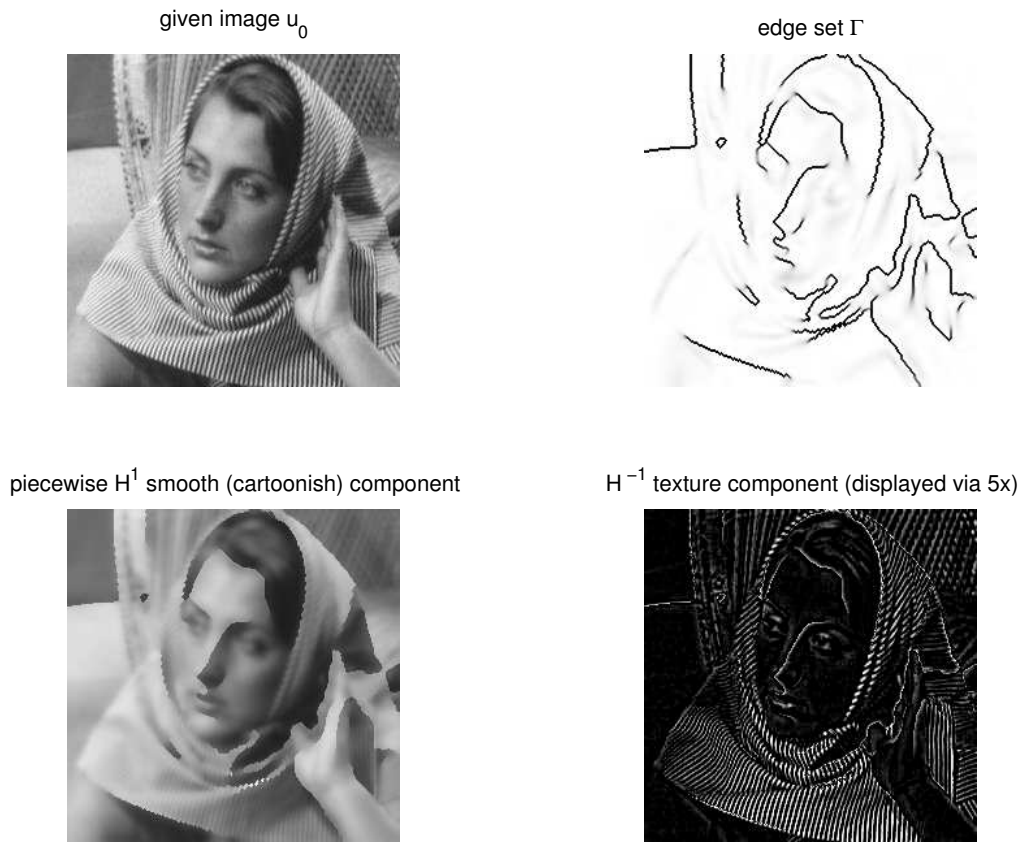

Figure 1: The performance of the proposed MSS model on a generic test image. The model may well simulate how a typical artist creates a painting u_0: first sketch the outlines Γ (upper right), followed by filling in the cartoonish overall shades u for each structure (lower left), and finally elaborate the detailed textures v (lower right) to bring complexion and life to the entire scene u_0.

4.3 Textures Do Contribute to Segmentation

We conclude this short research note by justifying the role of textures for segmentation.

In the classical Mumford-Shah model, segmentation is mainly brought out by the discontinuities of the Sobolev (or cartoonish) component u. We now argue that in the MSS model, the texture component v does indeed contribute to the segmenting process, as similarly performed by the human vision system. The following *simplified* analysis sheds some light on why this is the case.

Consider the 1-D image domain $\Omega = (-\pi, \pi)$, and a given oscillatory (and measurable) image

$$u_0(x) = \begin{cases} \sin(k_- x) & x \in \Omega_- = (-\pi, 0), \\ \sin(k_+ x) & x \in \Omega_+ = (0, \pi), \end{cases}$$

where the "wave numbers" k_- and k_+ are positive integers, and satisfy (see Fig. 2)

$$k_- \gg k_+ \gg 1. \tag{18}$$

Treat such an image as a *pure* texture distribution v. To human vision, it is natural to identify $x = 0$ as a boundary or edge point. We now investigate the quantitative effect of introducing $\Gamma = \{0\}$ as an edge point.

First assume that $\Gamma = \{0\}$ is indeed acknowledged as an edge point. Then $v = u_0$ is segmented into two components $v_\pm$ on each $\Omega_\pm$. Let $\Phi_\pm$ denote the corresponding texture potentials. Then one must have

$$-\Phi_\pm''(x) = v_\pm, \quad \Phi_\pm(z) = 0, \quad z \in \partial\Omega_\pm,$$

where $\pm$'s must be uniformly $+$ or $-$. Therefore, we have

$$\Phi_\pm = \frac{\sin(k_\pm x)}{k_\pm^2},$$

and

$$\|v\|^2_{H^{-1}(\Omega\setminus\Gamma)} = \int_{-\pi}^{0} |\Phi_-'(x)|^2 dx + \int_0^{\pi} |\Phi_+'(x)|^2 dx = \frac{\pi}{2}\left(\frac{1}{k_-^2} + \frac{1}{k_+^2}\right) = \frac{1}{8\pi}\left(\lambda_-^2 + \lambda_+^2\right), \tag{19}$$

where $\lambda_\pm = 2\pi/k_\pm$ denote the wavelengths. By the assumption in (18), $\lambda_- \ll \lambda_+ \ll 1$ (see Fig. 2).

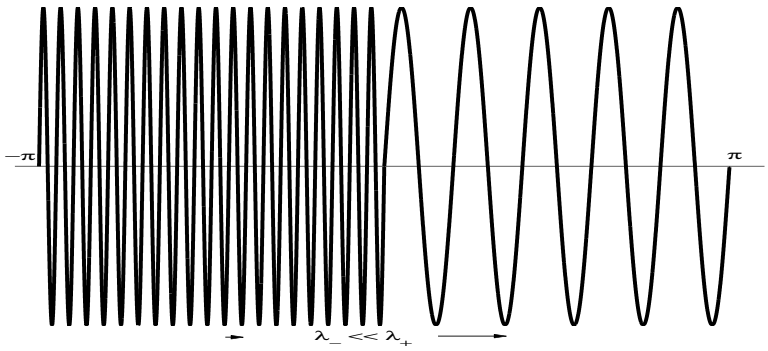

Figure 2: The example of piecewise harmonic waves for analyzing the role of H^{-1}–textures in segmentation. Notice the visually noticeable difference between the two wavelengths $\lambda_- \ll \lambda_+$.

Second, we investigate whether there could be a substantial energy increment when $\Gamma = \{0\}$ is *not* acknowledged as an edge point. Let Φ denote the texture potential of v on Ω. Then

$$-\Phi''(x) = v(x), \quad \Phi(-\pi) = \Phi(\pi) = 0.$$

Then one must have

$$\Phi(x) = \frac{\sin(k_\pm x)}{k_\pm^2} + a_\pm + b_\pm x, \quad x \in \Omega_\pm,$$

for some constants $a_\pm$ and $b_\pm$ to be determined next. The boundary conditions at $\pm\pi$ imply that one can rewrite the solution to

$$\Phi(x) = \frac{\sin(k_\pm x)}{k_\pm^2} + b_\pm(x \mp \pi), \quad x \in \Omega_\pm.$$

Since $v = u_0$ has been assumed to be a *measurable* function, to avoid the emerging of Dirac's delta measure at $x = 0$, one must now enforce the first-order continuity conditions:

$$\Phi(0^-) = \Phi(0^+), \quad \text{and} \quad \Phi'(0^-) = \Phi'(0^+).$$

Therefore, the two parameters are uniquely given by

$$b_+ = -b_- = \frac{1}{2}\left(\frac{1}{k_-} - \frac{1}{k_+}\right) = \frac{1}{4\pi}(\lambda_- - \lambda_+) = O(\lambda_+).$$

In particular, one observes that the long waves (with a large H^{-1}–norm) on Ω_+ have "penetrated" the middle point $x = 0$ and "polluted" the texture on Ω_-. Finally,

$$\int_{\Omega_\pm} |\Phi'(x)|^2 dx = \frac{1}{8\pi}\lambda_\pm^2 + \pi b_\pm^2 = \frac{1}{8\pi}\left(\lambda_\pm^2 + \frac{1}{2}(\lambda_+ - \lambda_-)^2\right),$$

and as a result, without introducing $\Gamma = \{0\}$ as an edge point, one would have

$$\|v\|_{H^{-1}(\Omega)}^2 = \frac{1}{8\pi}\left(\lambda_+^2 + \lambda_-^2 + (\lambda_+ - \lambda_-)^2\right) \tag{20}$$

In combination of (19) and (20), the relative (squared) energy increment when $\Gamma = \{0\}$ is *not* acknowledged as an edge point is

$$\frac{(\lambda_+ - \lambda_-)^2}{\lambda_+^2 + \lambda_-^2} \simeq 1,$$

since it has been assumed that the wavelengths satisfy $\lambda_+ \gg \lambda_-$.

To conclude, there arises a substantial (texture) energy increment if the visually meaningful boundary $\Gamma = \{0\}$ is not acknowledged. In terms of the original Mumford-Shah-Sobolev model, this increment, after being weighted by the parameter μ in the model, competes with the free-boundary energy ($\mathcal{H}^0(\Gamma)$ in the present 1-D case) in a more complex manner, which will be addressed in forthcoming works.

Acknowledgments

For their constant encouragement and inspirations, the author is profoundly thankful to Professors Gil Strang, Tony Chan, Stan Osher, David Mumford, and Jean-Michel Morel, as well as to his dear friends Professors Luminita Vese, Haomin Zhou, and Sung-Ha Kang.

References

[1] L. Ambrosio. A compactness theorem for a new class of functions of bounded variation. *Bollettino U. M. I.*, 7(3-B):857–881, 1989.

[2] L. Ambrosio and V. M. Tortorelli. On the approximation of free discontinuity problems. *Boll. Un. Mat. Ital.*, 6-B:105–123, 1992.

[3] G. Aubert and P. Kornprobst. *Mathematical Problems in Image Processing.* Springer-Verlag, 2001.

[4] J.-F. Aujol, G. Gilboa, T. F. Chan, and S. Osher. Structure-texture image decomposition-Modeling, algorithms, and parameter selection. *Preprint*, 2005.

[5] J.-F. Aujol and S.-H. Kang. Color image decomposition and restoration. *J. Visual Comm. Image Rep.,* to appear, 2005.

[6] A. Chambolle, R. A. DeVore, N.-Y. Lee, and B. J. Lucier. Nonlinear wavelet image processing: variational problems, compression and noise removal through wavelet shrinkage. *IEEE Trans. Image Processing*, 7(3):319–335, 1998.

[7] T. F. Chan and J. Shen. Variational restoration of non-flat image features: models and algorithms. *SIAM J. Appl. Math.*, 61(4):1338–1361, 2000.

[8] T. F. Chan and J. Shen. *Image Processing and Analysis: variational, PDE, wavelet, and stochastic methods.* SIAM Publisher, Philadelphia, 2005.

[9] T. F. Chan, J. Shen, and L. Vese. Variational PDE models in image processing. *Notices Amer. Math. Soc.*, 50:14–26, 2003.

[10] T. F. Chan and L. A. Vese. Active contours without edges. *IEEE Trans. Image Process.*, 10(2):266–277, 2001.

[11] T. F. Chan and L. A. Vese. A level set algorithm for minimizing the Mumford-Shah functional in image processing. *IEEE/Computer Society Proceedings of the 1st IEEE Workshop on "Variational and Level Set Methods in Computer Vision"*, pages 161–168, 2001.

[12] F. Cucker and S. Smale. On the mathematical foundations of learning. *Bull. AMS*, 39(1):1–49, 2001.

[13] G. Dal Maso, J.-M. Morel, and S. Solimini. A variational method in image segmentation: Existence and approximation results. *Acta. Math.*, 168:89–151, 1992.

[14] I. Daubechies. *Ten lectures on wavelets.* SIAM, Philadelphia, 1992.

[15] D. L. Donoho. De-noising by soft-thresholding. *IEEE Trans. Information Theory*, 41(3):613–627, 1995.

[16] D. L. Donoho and I. M. Johnstone. Ideal spacial adaption by wavelet shrinkage. *Biometrika*, 81:425–455, 1994.

[17] S. Esedoglu and J. Shen. Digital inpainting based on the Mumford-Shah-Euler image model. *European J. Appl. Math.*, 13:353–370, 2002.

[18] L. C. Evans. *Partial Differential Equations.* Amer. Math. Soc., 1998.

[19] L. C. Evans and J. Spruck. Motion of level sets by mean curvature. *J. Diff. Geom.*, 33(3):635–681, 1991.

[20] G. B. Folland. *Real Analysis - Modern Techniques and Their Applications.* John Wiley & Sons, Inc., second edition, 1999.

[21] S. Geman and D. Geman. Stochastic relaxation, Gibbs distributions, and the Bayesian restoration of images. *IEEE Trans. Pattern Anal. Machine Intell.*, 6:721–741, 1984.

[22] W. Gibbs. *Elementary Principles of Statistical Mechanics.* Yale University Press, 1902.

[23] E. De Giorgi, M. Carriero, and A. Leaci. Existence theorem for a minimization problem with free discontinuity set. *Arch. Rational Mech. Anal.*, 108:195–218, 1989.

[24] D. H. Hubel and T. N. Wiesel. Receptive fields, binocular intersection and functional architecture in the cat's visual cortex. *Journal of Physiology*, 160:106–154, 1962.

[25] E. H. Lieb and M. Loss. *Analysis.* Amer. Math. Soc., second edition, 2001.

[26] Y. Meyer. *Wavelets and Operators.* Cambridge University Press, 1992.

[27] Y. Meyer. *Oscillating Patterns in Image Processing and Nonlinear Evolution Equations*, volume 22 of *University Lecture Series.* AMS, Providence, 2001.

[28] J.-M. Morel and S. Solimini. *Variational Methods in Image Segmentation*, volume 14 of *Progress in Nonlinear Differential Equations and Their Applications*. Birkhäuser, Boston, 1995.

[29] D. Mumford. Elastica and computer vision. In C. L. Bajaj, editor, *Algebraic Geometry and its Applications*, pages 491–506. Springer-Verlag, New York, 1994.

[30] D. Mumford. *Geometry Driven Diffusion in Computer Vision*, chapter "The Bayesian rationale for energy functionals", pages 141–153. Kluwer Academic, 1994.

[31] D. Mumford and B. Gidas. Stochastic models for generic images. *Quaterly of Applied Mathematics*, 59:85–111, 2001.

[32] D. Mumford and J. Shah. Optimal approximations by piecewise smooth functions and associated variational problems. *Comm. Pure Applied. Math.*, 42:577–685, 1989.

[33] S. Osher and J. A. Sethian. Fronts propagating with curvature-dependent speed: Algorithms based on Hamilton-Jacobi formulations. *J. Comput. Phys.*, 79(12):12–49, 1988.

[34] S. Osher, A. Sole, and L. Vese. Image decomposition and restoration using total variation minimization and the H^{-1} norm. *UCLA CAM Tech. Report*, 02-57, 2002.

[35] L. Rudin and S. Osher. Total variation based image restoration with free local constraints. *Proc. 1st IEEE ICIP*, 1:31–35, 1994.

[36] L. Rudin, S. Osher, and E. Fatemi. Nonlinear total variation based noise removal algorithms. *Physica D*, 60:259–268, 1992.

[37] J. Shen. Inpainting and the fundamental problem of image processing. *SIAM News*, 36, 2003.

[38] J. Shen. On the foundations of vision modeling I. Weber's law and Weberized TV (total variation) restoration. *Physica D: Nonlinear Phenomena*, 175:241–251, 2003.

[39] J. Shen. Bayesian video dejittering by BV image model. *SIAM J. Appl. Math.*, 64(5):1691–1708, 2004.

[40] S. Smale and D.-X. Zhou. Shannon sampling and function reconstruction from point values. *Bull. Amer. Math. Soc.*, 41:279–305, 2004.

[41] J. L. Starck, M. Elad, and D. L. Donoho. Image decomposition via the combination of sparse representation and a variational approach. *IEEE Trans. Image Process.,* to appear, 2005.

[42] G. Strang. *Introduction to Applied Mathematics*. Wellesley-Cambridge Press, MA, 1993.

[43] G. Strang and T. Nguyen. *Wavelets and Filter Banks*. Wellesley-Cambridge Press, Wellesley, MA, 1996.

[44] A. N. Tikhonov. Regularization of incorrectly posed problems. *Soviet Math. Dokl.*, 4:1624–1627, 1963.

[45] L. A. Vese and S. J. Osher. Modeling textures with Total Variation minimization and oscillating patterns in image processing. UCLA CAM Tech. Report 02-19, May 2002.

[46] S. C. Zhu, Y. N. Wu, and D. Mumford. Minimax entropy principle and its applications to texture modeling. *Neural Computation*, 9:1627–1660, 1997.